Received: May 6, 2025 Revised: August 18, 2025 Accepted: September 2, 2025

https://doi.org/10.1016/j.neurom.2025.09.304

Selective Optogenetic Inhibition of Slow Conducting Fibers at the Level of the Sciatic Nerve Trunk in the Mouse

Mary G. Ardren, PhD[1,2]; Jerico V. Matarazzo, BSc[1,2]; Elise A. Ajay, PhD[1]; Alex C. Thompson, PhD[1,2]; Sophie C. Payne, PhD[1,2]; James B. Fallon, PhD[1,2]; Rachael T. Richardson, PhD[1,2]

ABSTRACT

Objective: Peripheral nerve stimulation is a drug-free alternative for chronic pain management, suppressing nociception through gating mechanisms in the spine. However, excitation through electrical stimulation does not easily discriminate between sensory and motor fibers or their functional subtypes, and can cause off-target effects. Targeted optogenetic inhibition may be a more selective method to suppress nociceptive activity directly while leaving neighboring fibers unaffected.

Materials and Methods: In this study, the chloride-specific light-gated ion pump halorhodopsin (enhanced *Natronomonas* halorhodopsin [eNpHR]) was introduced into the sciatic nerve of eight adult C57BL/6 mice through intrasciatic injection of adeno-associated virus 6-hSyn-eNpHR–enhanced yellow fluorescent protein (eNpHR-eYFP). After three to four weeks, an acute electrophysiological study was performed to assess optical inhibition of slow conducting electrically evoked compound action potential (eCAP) activity using light directed to the main nerve trunk. Immunohistochemical characterization of eNpHR-eYFP expression was performed in L3–L5 dorsal root ganglion (DRG) neurons.

Results: eNpHR-eYFP was detected in the cell bodies and axons of a subset of DRG neurons (~7%), with soma size and expression pattern consistent with nociceptors (75% of eNpHR-eYFP cells have a soma size of ≤267 μm^2). The amplitude of slow velocity eCAPs (mean conduction velocity 0.6 m/s) was significantly reduced in the presence of yellow light (~20% reduction; Wilcoxon signed-rank test, $p = 0.008$). The amplitude of fast- (22 m/s) and medium- (6 m/s) conducting eCAPs was not affected.

Discussion: This study extends the current understanding of using light-mediated inhibition of nociceptive activity in a mixed peripheral nerve to the level of the axon and measures the underlying changes in neural activity in the sciatic nerve. This study provides evidence for selective light-mediated inhibition at the site of the axon, with potential applications for the suppression of chronic pain.

Keywords: Chronic pain, neuromodulation, nociception, optogenetic inhibition, peripheral nerve stimulation

INTRODUCTION

Pain perception in the upper and lower extremities can be modulated by applying electrical stimulation to associated peripheral nerves through implanted or transcutaneous devices.[1–3] When delivered at a low frequency (40–100 Hz), the stimulation causes an abnormal sensation known as paresthesia and reduces pain signaling indirectly through spinal gating mechanisms.[4] The stimulation is intended to target non-nociceptive (Aα and Aβ) fibers that activate inhibitory interneurons in the dorsal horn,[5,6] but incidental activation of motor fibers with similar excitability thresholds can cause spasms and cramping. Thus, the stimulating current must be capped, potentially limiting the therapeutic impact. Alternatively, high-frequency stimulation (in the kilohertz range) can more readily achieve paresthesia-free pain relief through neural desensitization or conduction block.[7,8] Here, the modulation targets are the nociceptive C and Aδ fibers, but targeting these fibers is challenging, and the stimulation can affect the level and quality of tactile sensation and muscle strength.[9]

Optogenetics is an alternative approach to electrical neuromodulation, wherein light is used to control activity in neurons that are genetically modified with light-sensitive proteins called opsins.[10] Opsins can be excitatory, such as the cationic channelrhodopsin-2 (ChR2) first isolated from *Chlamydomonas reinhardti*,[11] or inhibitory, such as the halorhodopsin chloride pump from *Natronomonas pharaonis* (enhanced *Natronomonas*

Address correspondence to: Mary G. Ardren, PhD, The Bionics Institute of Australia, Daly Wing, St Vincent's Hospital, Level 7, 35 Victoria Parade, Fitzroy 3065, Victoria, Australia.

[1] Bionics Institute, Fitzroy, Victoria, Australia; and
[2] The University of Melbourne, Medical Bionics Department, Parkville, Australia

For more information on author guidelines, an explanation of our peer review process, and conflict of interest informed consent policies, please see the journal's Guide for Authors.

Source(s) of financial support: This work was supported by The CASS Foundation and the Bionics Institute Incubator Fund. The Bionics Institute acknowledges the support it receives from the Victorian Government through the operational infrastructure program.

halorhodopsin [eNpHR]).[12] Superior selectivity of optogenetic neuromodulation to that of electrical stimulation is achieved by confining expression of opsins in specific neuronal types through targeted injection, cell-specific promoters, or natural tropism of adeno-associated virus (AAV) serotypes.[13–15]

A fundamental advantage of optogenetics over electrical stimulation is selective inhibition of neural activity that may be used as a direct method of suppressing nociceptive activity without interfering with normal touch sensation. Previous studies have shown that transdermal excitation of eNpHR or other light-gated potassium ion channels selectively expressed in nociceptive fibers of the sciatic nerve reduces the perception of pain in mice as measured by behavioral assays.[16–18] Although these studies provide an exciting foundation for pursuing this direct and selective route for managing chronic pain, these studies did not extend their investigations to an in vivo electrophysiology study. Understanding the neural responses underlying these behavioral changes (eg, nerve ending inhibition) is an important research area for developing clinically implementable treatments. Moreover, transdermal light delivery is likely to prevent initiation of activity, rather than interrupt existing nociceptive activity traveling to the central nervous system. Transdermal light delivery also is less suitable for addressing pain that originates from nondermal nociceptors, such as leg or back pain, or for larger dermal regions of pain. As such, an implanted device that delivers light to the nerve trunk is needed for versatile pain suppression to more regions of the body.

The aim of this study was to determine whether light directed to the nerve trunk selectively suppresses the activity of nociceptors in mice expressing an inhibitory opsin in C fibers of the sciatic nerve, as recorded using in vivo electrophysiology. In naïve mice, AAV6-hSyn-eNpHR-enhanced yellow fluorescent protein (eYFP) (from here on referred to as eNpHR-eYFP) was injected into the left sciatic nerve, with intrasciatic delivery chosen as an established method for opsin delivery, with high clinical applicability.[15,17,19,20] After three to four weeks, the threshold and amplitude of electrically evoked compound action potentials (eCAPs) were measured in the presence or absence of amber light applied to the sciatic nerve of anesthetized mice. The expression of eNpHR in dorsal root ganglion (DRG) neurons also was characterized through immunohistochemistry, using the eYFP fluorophore, NeuN as an all-cell marker, and neurofilament 200 (NF200) and calcitonin gene-related peptide (CGRP) as markers of large-diameter fibers and peptidergic nociceptors, respectively.[21]

MATERIALS AND METHODS

Ethics Approval

All procedures using animals were approved by the St Vincent's Hospital (Melbourne, Australia) Animal Ethics Committee (reference: #001/23). This study complies with the *Guidelines to Promote the Wellbeing of Animals used for Scientific Purposes* (2013), the *National Health and Medical Research Council Code for Care and Use of Animals for Scientific Purposes* (eighth edition, 2013, updated 2021), and the Prevention of Cruelty to Animals Amendment Act (2015).

Animals

C57BL/6 mice were purchased from the Walter and Eliza Hall Institute (Melbourne, Australia). Male and female C57BL/6 mice (four to six weeks old) were housed under a 12-hour light/dark cycle. Food and water were available ad libitum.

Adeno-associated Virus

AAV6 was chosen owing to its described specificity for nociceptive neurons after intrasciatic injection.[15,17] AAV6-hSyn1-ChR2 (H134R)-mCherry (ChR2-mCherry) and AAV6-hSyn1-eNpHR3.0-eYFP (eNpHR-eYFP) were chosen for excitation and inhibition, respectively. The vectors, packaged by VectorBuilder (Chicago, IL), were prepared at 1×10^{13} genomic copies/mL in phosphate buffered saline (pH7.4), supplemented with 200 mM sodium chloride and 0.001% pluronic F-68. All viruses were stored in −80 °C freezer and thawed ≤five days before injection. Before injection, all viruses were mixed with fast green FCF (Sigma-Aldrich, St Louis, MO) to a final concentration of 1% (weight/volume) for confirmation of virus uptake in the nerve.

Intrasciatic Virus Injection

All procedures were performed under general anesthesia. Mice were placed in a sealed chamber, and anesthesia was induced using 1.5% to 3% isoflurane and oxygen delivered at a flow rate between 1.5 and 3 L/min. After confirmation of deep anesthesia, mice were moved to a heating pad kept at 37 °C, and anesthesia was maintained using 1.5% to 2% isoflurane in oxygen delivered through a nose cone at 1.5 L/min. The eyes were covered with a thin layer of Viscotears liquid gel (Alcon, Camberley, UK). Mice received buprenorphine (0.05–0.1 mg/kg, subcutaneous; SC) as a local analgesic, and carprofen (5 mg/kg, SC) to relieve postsurgical inflammation. Depth of anesthesia was monitored using respiratory rate. Surgery commenced after the loss of response to a toe-pinch test.

All surgical procedures were performed using aseptic techniques.[22] Briefly, a 1-to-2 cm incision over the main trunk of the left sciatic nerve (mid-thigh level) was accomplished using forceps and a scalpel, and the biceps femoral muscle was detached from the gluteus superficialis to expose the distal region of the sciatic nerve.[23] The sciatic nerve was dissected from the surrounding fascia using blunt forceps. Virus injections were performed using a filamented quartz glass capillary (0.7/1 mm inner/outer diameter; #QF100-70-10, Sutter Instrument Company, Novato, CA), pulled to a fine tip micropipette (P-2000, Sutter Instrument Company). Micropipettes were inserted into the micropipette holders attached to a 10-µL Hamilton syringe connected to a micropump (UltraMicroPump III, World Precision Instruments, Sarasota, FL). Loaded micropipettes were inserted under the epineurium of the main trunk of the exposed sciatic nerve (proximal to the common peroneal and tibial branch points), and 4 to 6 µL of virus was injected at one to two sites at 1 µL/min (total $4–6 \times 10^{10}$ genomic copies delivered). Care was taken to limit handling of the nerve as much as possible. After injection, the needle was left in place for 30 seconds to equilibrate the liquid and prevent backflow.[24] The muscles and skin were sutured together using absorbable 7-0 sutures (Ethicon, Raritan, NJ). Mice were left to recover on a heating blanket and received high-calorie boost hydrogel (ClearH_2O, Westbrook, ME) after surgery.

Sciatic Electrode Array Design

An in-house designed nerve cuff contained three pairs of opposing platinum electrodes, with the distance between electrode pairs being 3.4 mm.[25] Each electrode had an exposure surface area of 0.39 mm^2 and was encased in transparent medical grade silicone. The electrodes of the distal and proximal pairs were offset, such that they were adjacent, and the electrodes of the central pair were directly opposing (Fig. 1). The cuff contained a channel for the nerve

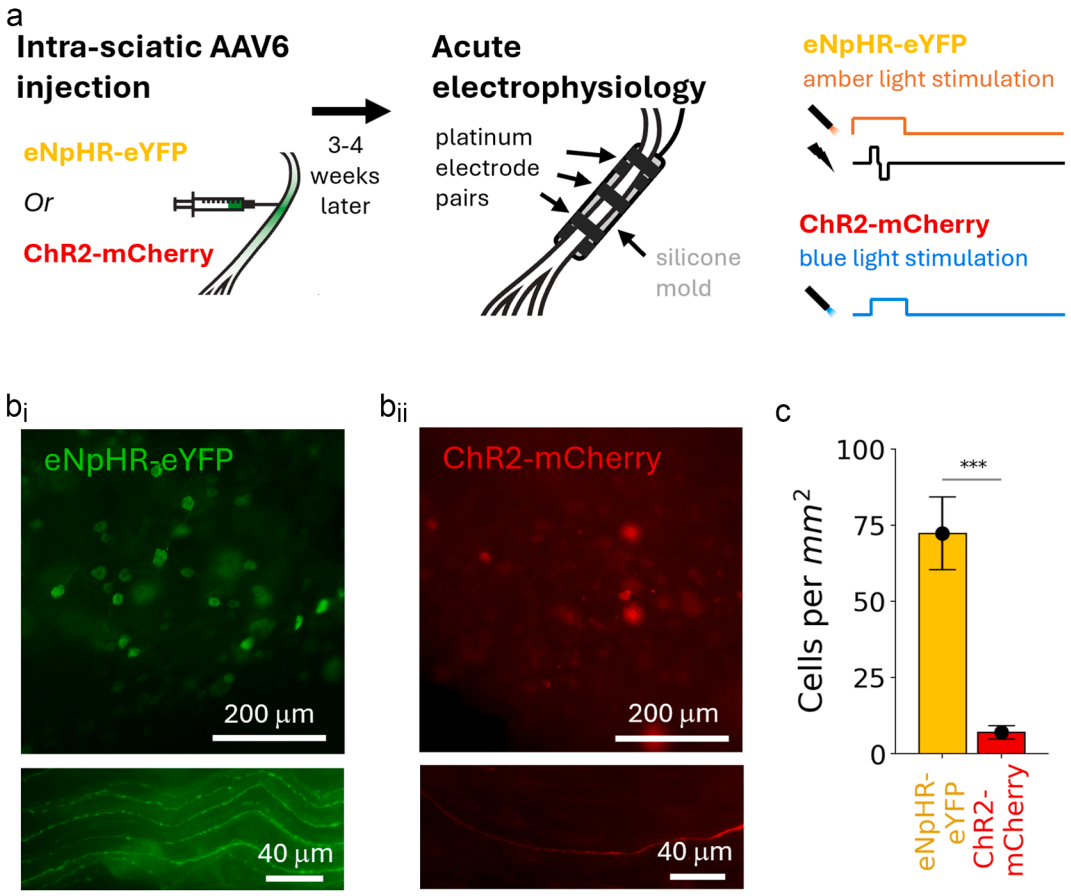

Figure 1. Schematic of experimental design and overall expression of opsins. a. Intrasciatic injection of AAV6 for opsin delivery (left panel). Three to four weeks later, mice underwent acute electrophysiology experiments using a sciatic nerve cuff to evoke and record neural activity (middle panel). Mice injected with eNpHR-eYFP were stimulated using electrical stimulation coupled with pulses of amber light to cause inhibition of electrically evoked neural activity (upper right panel). Those injected with ChR2-mCherry were stimulated using pulses of blue light to cause activation (lower right). b. Example of whole mount DRG (top panel) and sciatic nerve (bottom panel) tissue from a single animal showing expression eNpHR-eYFP (b_i) or ChR2-mCherry (b_{ii}). c. Bar graph showing mean number of opsin-positive cells per mm^2 from randomly selected L3-L5 DRG sections (ChR2-mCherry: $n = 8$ sections, eNpHR-eYFP: $n = 15$ sections). Closed circles indicate mean; error bars indicate SEM; $^{***}p < 0.001$, independent *t*-test. [Color figure can be viewed at www.neuromodulationjournal.org]

and was designed to apply a slight deformative pressure to the nerve for optimal stimulation and recording.[26]

Acute Electrophysiology

Three to four weeks after injection, mice were anesthetized for a final non-recovery experiment (1% to 3% isoflurane as previously described). The region of the sciatic nerve that received the injection was identified and dissected away from surrounding tissue to expose 8 to 10 mm length of the nerve between the distal branch points of the common peroneal, tibial, and sural nerves, and the proximal notch. After encasing the nerve with the electrode array (with the site/s of injection embedded within), the cuff was sutured closed to keep the nerve immobile within the channel. Warm Hartmann's fluid was applied to the exposed tissue to maintain moisture throughout the recording period.

Impedance Testing and Electrical Stimulation

Common Ground Impedance

Common ground impedance for each electrode was measured from end-of-phase voltage transients during current pulses (100-µs phase width, 25-µs interphase gap at 100-µA current), in common-ground configuration (one active electrode vs all others as return), and visualized using IGOR Pro-9 (Wavemetrics, Portland, OR).

Electrical Stimulation

Biphasic stimulation (4–20 Hz, 50–300 µs pulse width, 8–50 µs interpulse gap, 0–2 mA current, alternating cathodic/anodic polarity) was delivered to the distal or middle pair of electrodes through a custom-made stimulator.[27]

Optical Stimulation

For those mice expressing ChR2-mCherry, light stimuli were delivered using a custom 452 nm solid state laser (Optotech, Southbank, Australia) coupled to a 105 µm core optical fiber (numerical aperture of 0.22) by an fiber-optic connector. The cleaved end of the optical fiber was positioned 0.5 to 2 mm distal to the recording electrodes to optically stimulate the tissue. The optical fiber was positioned at 1 mm above the sciatic nerve to deliver a spot size with diameter 441 µm. Blue-light pulses were 1 to 5 milliseconds in duration at 0 to 13.9 mW intensities.[22,28]

For those mice expressing eNpHR-eYFP, light stimuli were delivered by a 595 nm light-emitting diode (M595F2, Thorlabs, Newton, NJ) coupled to a 200 μm core optical fiber (numerical aperture of 0.22) using a SubMiniature version A connector. The optical fiber was positioned at 1 mm above the sciatic nerve to deliver 537 μm diameter spot size amber light between the stimulating electrodes and the closest recording electrodes. Amber light pulses were 3 to 5 milliseconds in duration at 0 to 3.3 μW intensities.

The light sources were calibrated using a photodiode (PDA36A2, Thorlabs) coupled through an optical fiber. Either blue or amber light was delivered alone or paired with electrical stimulation.

Evoked Nerve Recording Data Acquisition

Compound action potentials (CAPs) evoked by bipolar eCAP or optical (oCAP) stimulation were recorded from the proximal pair of electrodes.[29] CAPs were acquired using an isolated differential amplifier with an active probe (ISO-80, World Precision Instruments) and sampled at 200 kHz using a data acquisition device (USB-6210, National Instruments, Austin, TX) and digitally filtered at 110 to 2000 Hz (infinite impulse response bandpass filter). CAP recordings were evoked at 4 to 20 Hz and averaged over >20 trials, with two recording block repeats per stimulating configuration. eCAPs were performed first to identify thresholds for electrically evoked neural subclasses of fibers (based on latency) and myogenic activity (which were visually confirmed). For those mice expressing ChR2-mCherry, oCAPS were then performed to confirm presence and function of the excitatory opsin. In some animals, yellow-light stimulation was applied to the injected nerve during recording, and/or blue-light stimulation was applied on the non-injected right side during recording as controls. For those mice expressing eNpHR-eYFP, suppression of slow conducting neural activity was assessed using amber-light stimulation (activation of eNpHR) during eCAPs. Slow conducting C-fiber responses were visually confirmed in each animal, and parameters used to elicit C-fiber activity were noted before the application of amber light.

Evoked Nerve Recording Data Analysis

Data analysis was performed offline using custom code in IGOR Pro-9 software. To reduce the impact of artifact during electrical stimulation, traces were averaged over alternating stimulation polarities. Thresholds for electrical or optical stimulation were estimated as the minimum stimulus intensity producing a response amplitude ≥0.1 μV above background and visually confirmed by the experimenter. For oCAPs, peak-to-peak amplitudes of responses generated from a 2 millisecond pulse of blue light at increasing light intensities were taken (5 millisecond window of analysis starting 1 millisecond after light stimulation). Mean conduction velocity was estimated using the latency to slowest peak response from stimulation onset and the distance between optical fiber and recording electrodes. For eCAPs, peak-to-peak amplitudes of responses generated from 50 to 300 μs pulse of electrical stimulation at increasing current intensities were measured.

Tissue Preparation for Histology

At the conclusion of the experiment, mice were euthanized through intraperitoneal injection of 300 mg/kg pentobarbitone sodium (Lethabarb, Virbac, Milperra, Australia). After cessation of respiration, mice were intracardially perfused with warm saline solution followed by 10% neutral buffered formalin (Sigma-Aldrich). The left sciatic nerve (the length of the nerve containing the injection site and electrode array implant) and L3–L5 DRGs were removed and postfixed for 24 to 48 hours at 4 °C. Tissue was then washed and stored in phosphate buffered saline (PBS). Tissue was cryoprotected in 30% sucrose before being embedded in optimal cutting temperature compound (Tissue-Tek, Sakura, Japan) and sectioned at 12 μm at −20 °C using a CryoStar NX70 Cryostat (Erpedia, Kalamazoo, MI).

Immunohistochemistry

Slides with sections of L3–L5 DRG tissue were washed twice in PBS and blocked for three hours at room temperature in PBS containing 2% (volume/volume [v/v]) donkey serum and 0.3% (v/v) Triton X-100 ("blocking solution"). Primary antibodies (diluted in blocking solution) were incubated overnight at 4 °C and included chicken antineurofilament 200 (NF200; 1:200, AB5539, Merck Millipore, Macquarie Park, Australia), goat anticalcitonin gene-related peptide (CGRP; 1:200, 1720–9007, BioRad, Hercules, CA), or rabbit antineuronal nuclei (NeuN; 1:1000, AB177487-1001, Abcam, Cambridge, UK). The following day, sections were washed in PBS three times before incubation in fluorescent secondary antibodies for three hours at room temperature. Secondary antibodies (also diluted in blocking solution) included AlexaFluor donkey anti-chicken 647 (1:500, A78952, Thermo Fisher Scientific, Waltham, MA), AlexaFluor donkey antigoat 594 (1:500, A11058, Thermo Fisher Scientific) and AlexaFluor donkey antirabbit 647 (1:500, A31573, Thermo Fisher Scientific). Sections were washed in PBS three times before coverslipping with Vectorshield antifade mounting media (Vector Laboratories, Newark, CA).

Imaging and Image Analysis

Sectioned DRGs were imaged using a Zeiss Axioplan II microscope (Carl Zeiss Microscopy, Jena, Germany) and AxioVision Software (Zeiss, White Plains, NY). For each section, images were taken using a z-stack (0.55 to 1 μm step intervals) and tiled to include the entire DRG section for analysis. Tiled images were stitched together using a selected channel for reference using AxioVision Software.

Stitched images were loaded into ImageJ (Rasband, W.S., ImageJ, US National Institutes of Health, Bethesda, MD) and separated into channels, and a maximum projection was applied to each channel. Thresholding was used to differentiate features of interest from background, adjusting the minimum threshold to the top 1% to 15% of values. Cell counts and soma size measurements were obtained from one to two DRGs per animal (L3, L4, L5). NeuN+, NF200+, CGRP+, and opsin+ cells were counted to determine percentage of opsin expression (as a total of all NeuN+ cells), in addition to functional subtype (opsin colocalization with NF200+ and CGRP+).[17,22]

Statistical Analysis

Differences in immunohistochemistry measurements were assessed using independent *t*-tests. After tests for normality (threshold at $p = 0.05$), differences in paired eCAP and oCAP recordings were assessed using either parametric paired *t*-tests or nonparametric Wilcoxon signed-rank tests. Similarly, differences in independent eCAP and oCAP recordings were assessed using parametric *t*-tests or nonparametric Mann-Whitney U rank tests.

Correlation between opsin expression and CAP measurements were assessed using the Pearson correlation coefficient.

RESULTS

Two cohorts of mice were used to evaluate delivery and function of opsins in nociceptors of the sciatic nerve (Fig. 1a). In the first cohort, eight mice (50% male) were injected with an AAV to deliver the inhibitory eNpHR-eYFP to evaluate light-mediated suppression of electrically evoked slow conduction velocity activity in the sciatic nerve. A second batch of eight mice (50% male) were injected with the excitatory opsin ChR2(H134R)-mCherry using a matched viral vector to further characterize the electrophysiological properties of the transduced fibers. Opsin expression was confirmed in L2–L5 DRG cell bodies (Fig. 1$b_{i,\ ii}$ upper panel), and within the axons contained within the main trunk of the sciatic nerve (the location of virus delivery and light stimulation; Fig. 1$B_{i,\ ii}$ lower panel). Notably, eNpHR-eYFP was expressed at a significantly higher rate in DRG cell bodies, with an average of 72 cells per mm^2 of DRG section ($n = 15$ [one–two sections per mouse, eight mice]) compared with seven cells per mm^2 of DRG sections in those injected with ChR2(H134R)-mCherry ($n = 8$ [one section per mouse, eight mice]; ***, independent t-test, $p = 0.0008$; Fig. 1c).

Selective Expression of Opsin in Small-Diameter Neurons

To quantify and characterize opsin expression in DRG cell bodies and sciatic axons, we visualized opsin expression through the covalently attached fluorophores (eYFP or mCherry), whereas neuronal cell types within the DRG were identified with a variety of antibodies.

For AAV6-hSyn1-eNpHR3.0-eYFP-injected animals, eNpHR-eYFP was detected in 7% ± 1% of all NeuN+ cells ($n = 15$ [one to two sections per mouse, eight mice]; Fig. 2a,e right). The mean soma size of eNpHR-eYFP cells was 236.7 ± 5.6 μm^2 ($n = 419$ cells), whereas the mean soma size of the overall NeuN population was 419.2 ± 4.9 μm^2 ($n = 2880$ cells). Unfortunately, however, NeuN was not detectable in approximately half of eNpHR-eYFP cells (Fig. 2e, left). There was no significant difference in soma size between NeuN+ and NeuN-negative eNpHR-eYFP cells (*ns*, independent t-test, $p = 0.057$; Table 1), pointing to NeuN as an ineffective all-cell marker. The soma size of 75% of eNpHR-eYFP positive cells was ≤267 μm^2, lower than the 75th percentile for identified cell types: 545 μm^2 for NeuN+, 729 μm^2 for NF200+, and 478 μm^2 for CGRP+ cells (Fig. 2d); 27.8% of all small diameter neurons (<200 μm^2) expressed eNpHR-eYFP. Table 1 summarizes the coexpression of opsin and antibodies used (see also Fig. 2e).

For those animals injected with AAV6-hSyn1-ChR2(H134R)-mCherry, the overall expression of ChR2-mCherry was tenfold lower, with <1% of all cells expressing ChR2-mCherry. The mean cross-sectional diameter of ChR2-mCherry positive cells was significantly smaller (mean soma size = 181.9 ± 9.7 μm^2, $n = 39$ cells, $n = 8$ [one section per mouse, eight mice]) than eNpHR-eYFP positive cells (**, independent t-test, $p = 0.004$; Fig. 2f).

Selective Activation of Slow Conduction Velocity Fibers Using Excitatory Opsins

For those animals injected with the ChR2-mCherry viral vector, blue-light stimulation of the injected sciatic nerve elicited a single-peak oCAP response, which was light-intensity dependent (Fig. 3a, b). The lowest light power able to elicit a neural response (light threshold) was 5 ± 0 mW ($n = 8$ mice). Compared with a no-light baseline, that is, noise floor (peak–peak amplitude = 1.3 μV ± 0.2 μV), the response amplitude at light-threshold was 2.9 μV ± 0.4 μV (significantly higher than baseline; *, $p = 0.016$; Wilcoxon signed-rank test), with 3 dB suprathreshold (or max light, 13.9 μW) intensity increasing the response amplitude from threshold to 5.6 μV ± 1.1 μV (**, $p = 0.008$, Wilcoxon signed-rank test; Fig. 3b). There was no correlation between peak-to-peak amplitude and number of mCherry positive cells counted per DRG (*ns*, $p = 0.144$, Pearson correlation coefficient).

Using distance between the optical fiber and the recording electrode pair, conduction velocity was calculated as 0.29 ± 0.1 m/s at light-threshold (not significantly different from 3 dB suprathreshold (or max light) conduction velocity at 0.31 ± 0.1 m/s; *ns*, $p = 0.546$, Wilcoxon signed-rank test, Fig. 3c).

Max amber-light (3 μW) stimulation of the ChR2-injected tissue did not produce any detectable response (1.8 μV ± 0.2 μV; $n = 2$ mice; *ns* from baseline, $p = 0.267$; Mann-Whitney U rank test; Fig. 3d). Similarly, max blue-light stimulation of noninjected sciatic tissue did not produce any detectable responses (2 μV ± 0.4 μV; $n = 2$ mice; *ns* from baseline, $p = 0.267$; Mann-Whitney U rank test; Fig. 3e).

Nonselective Activation of Fibers Using Electrical Stimulation

Before evaluating light-mediated inhibition, a study of eCAPs generated at two distances from recording electrodes was performed. For mice in both eNpHR-eYFP and ChR2-mCherry cohorts, electrical stimulation of the sciatic nerve elicited multipeak responses at varying latencies (Fig. 4). Fast neural responses and myogenic responses were initiated at lower charge levels (Fig. 4a, b), whereas slower propagating responses were only detectable using larger total charge (higher duration and current intensities; Fig. 4c and Supplementary Data Table S1).

Long distances (6.8 mm) between stimulating and recording electrodes were necessary to separate fast neural responses from electrical artifact (mean conduction velocity = 22 ± 4.2 m/s), whereas shorter distances (3.4 mm) were required to isolate medium velocity neural responses (6.2 ± 1.5 m/s). Slow velocity (0.6 ± 0.1 m/s) and myogenic activity were detected when recording at both long and short distances from the stimulating electrodes. There was no difference in the amplitude or conduction velocity between slow velocity responses elicited at 6.8 mm and 3.4 mm (Supplementary Data Table S1).

Fast (22 m/s), medium (6 m/s), and slow (0.6 m/s) conducting fiber types were comparable to reported conduction velocities from identified murine DRG neurons ([fast Aβ fibers = 24 m/s, medium Aδ fibers = 6 m/s, and slow C fibers 0.3 m/s] from Ruscheweyh et al[30]; Fig. 4d). Grouped by conduction velocity, there was an expected graded increase in the minimum charge required for recruiting fast to slow fibers (Fig. 4d, *, $p = 0.018$, one-way analysis of variance).

Selective Inhibition of Electrically Evoked Slow Wave Fibers Using Inhibitory Opsins

To evaluate the effect of light on the amplitude and latency of electrically evoked activity in eNpHR-modified fibers, activity in fast, medium, and slow conducting fibers was elicited through electrical stimulation in the presence and absence of a 3-to-5 millisecond pulse of amber light. Example recording traces from one mouse during electrical-only stimulation in the absence or

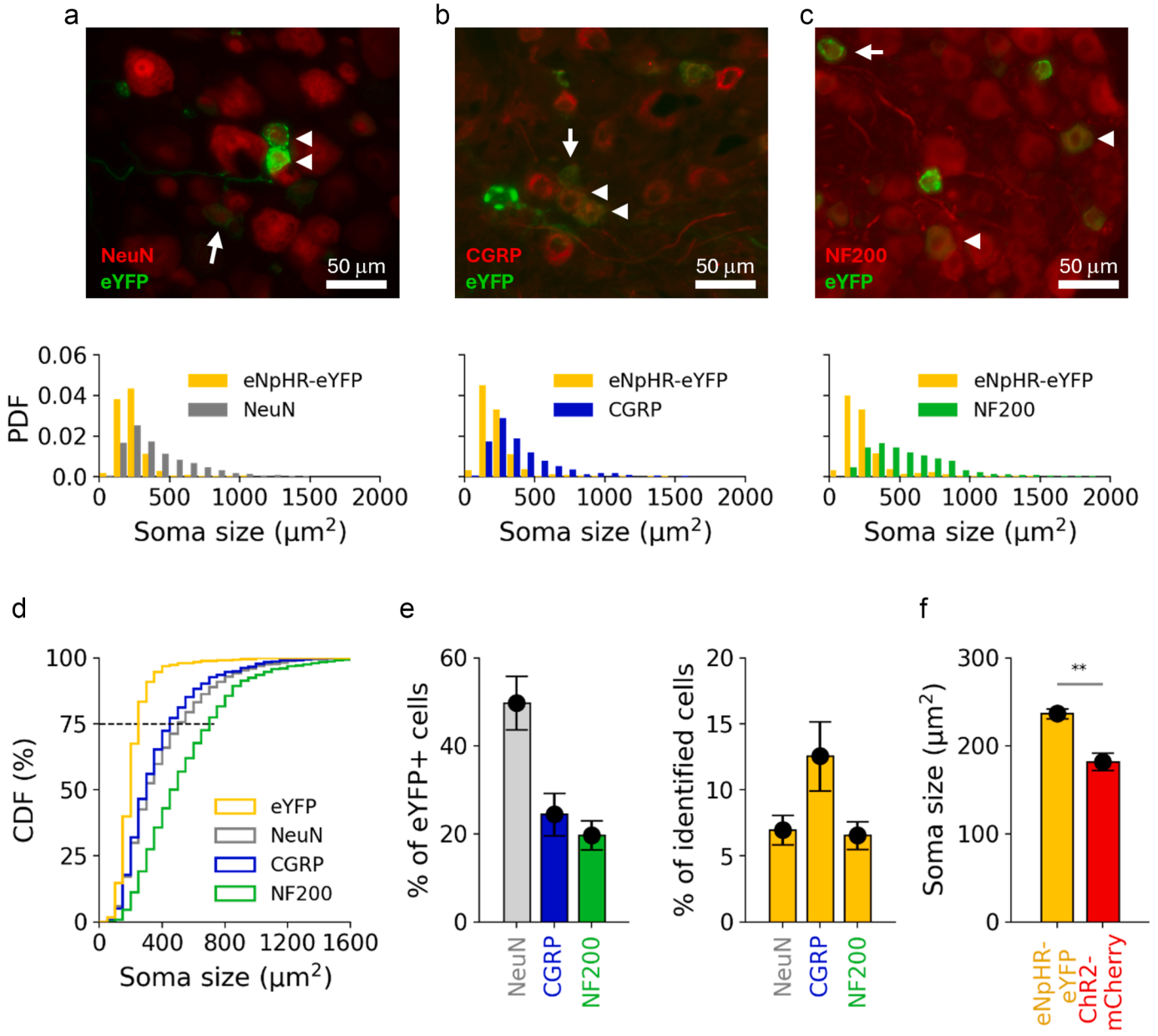

Figure 2. Expression of opsins in small-diameter DRG neurons. Example images showing expression of eNpHR-eYFP (arrow) and coexpression (arrowhead) with the neuronal marker NeuN (a), peptidergic neuron marker CGRP (b), mechanoreceptor marker NF200 (c), in separate DRG sections (upper panel). Probability distribution function (PDF; lower panel) showing distribution of soma size of eNpHR-eYFP+ and antibody positive cells (summary data, $n = 8$ animals). d. Cumulative distribution functions (CDF) of data shown in (a–c lower panel). e. Bar graph showing percentage of eNpHR-eYFP positive cells coexpressing with antibodies (left) and percentage of antibody identified cells expressing eNpHR-eYFP (right). f. Bar graphs of average soma size of opsin positive cells. Closed circles indicate mean; error bars indicate SEM; $^{**}p < 0.01$, independent *t*-test. PDF, probability distribution function. [Color figure can be viewed at www.neuromodulationjournal.org]

presence of amber light are shown in Figure 5a. To evaluate this, response threshold, peak-to-peak amplitudes, and conduction velocity for fast conducting, myogenic, and slow conducting fiber activity were determined (Fig. 5b).

Although there was no effect of light on fast or medium fibers or the recruitment of myogenic activity, slow conducting eCAP threshold was higher in the presence of amber light (electrical only = 968.8 ± 126.4 μA; amber light = 1050 ± 148.8 μA; $n = 8$ animals; *, $p = 0.042$, paired *t*-test; Fig. 5c$_i$). Furthermore, the peak-to-peak amplitude at electrical threshold was reduced in the presence of amber light (electrical only = 5.9 μV ± 1.6 μV; amber light = 4.8 μV ± 1.6 μV; **, $p = 0.008$, Wilcoxon signed-rank test), although it was comparable at 3 dB suprathreshold electrical stimulation (electrical only = 10 μV ± 2.7 μV; amber light = 10.1 μV ± 2.5 μV; *ns*, $p = 1.0$, Wilcoxon signed-rank test; Fig. 5c$_{ii}$). There was no difference in reduction of amplitude (as a percentage) between at-threshold slow velocity responses recorded at 6.8 mm (12%) or 3.4 mm (27%) from the stimulus (*ns*, $p = 0.26$, independent *t*-test; data not shown). There

Table 1. Coexpression of Opsin and Antibodies, With Percentage and Soma Size of Identified Neurons.

Marker	Coexpression	Percentage of cells	Soma size (μm^2)
eNpHR–eYFP +	NeuN +	50%	264.2 ± 23.8
	NeuN −	50%	210.1 ± 13.1
	CGRP +	24%	250.1 ± 21.1
	NF200 +	20%	394.3 ± 42.7
	CGRP + NF200 +	9%	279.3 ± 34.5
	CGRP − NF200 −	59%	207 ± 22.6
NeuN +	eNpHR-eYFP −	93%	437.7 ± 24.8
CGRP +	eNpHR-eYFP −	87%	363.9 ± 14.3
NF200 +	eNpHR-eYFP −	93%	559.7 ± 25.2

also was no effect of amber light on the conduction velocity of the response at respective thresholds (electrical only = 0.64 ± 0.06 m/s; amber light = 0.63 ± 0.06 ms; *ns*, $p = 0.453$, paired *t*-test; Fig. 5c$_{ii}$).

There was no correlation between histologically determined expression of opsin and threshold change (*ns*, $p = 0.76$, Pearson correlation coefficient) or difference in peak-to-peak amplitude (*ns*, $p = 0.86$, Pearson correlation coefficient). In addition, there was no difference in threshold change between male and female mice (*ns*, $p = 0.38$, independent *t*-test) or difference in peak-to-peak amplitude (*ns*, $p = 0.87$, independent *t*-test).

DISCUSSION

This study explores the feasibility of direct optogenetic inhibition of nociceptive activity at the level of the axon in the mouse sciatic nerve after genetic manipulation. Using intrasciatic injection of an AAV6 serotype viral vector, a proportion of small-diameter DRG neurons and their axons were selectively targeted to express the inhibitory eNpHR opsin. After the application of pulses of electrical stimulation to nonselectively activate all fiber types in the sciatic nerve of anesthetized mice, amber-light stimulation applied at the main trunk of the sciatic nerve was shown to selectively suppress electrically evoked slow velocity eCAPs. These results indicate that an optogenetic approach for selective inhibition of slow conducting activity combined with simultaneous neural recordings allows continued monitoring and direct suppression of nociceptive activity in the periphery, before it reaches the central nervous system.

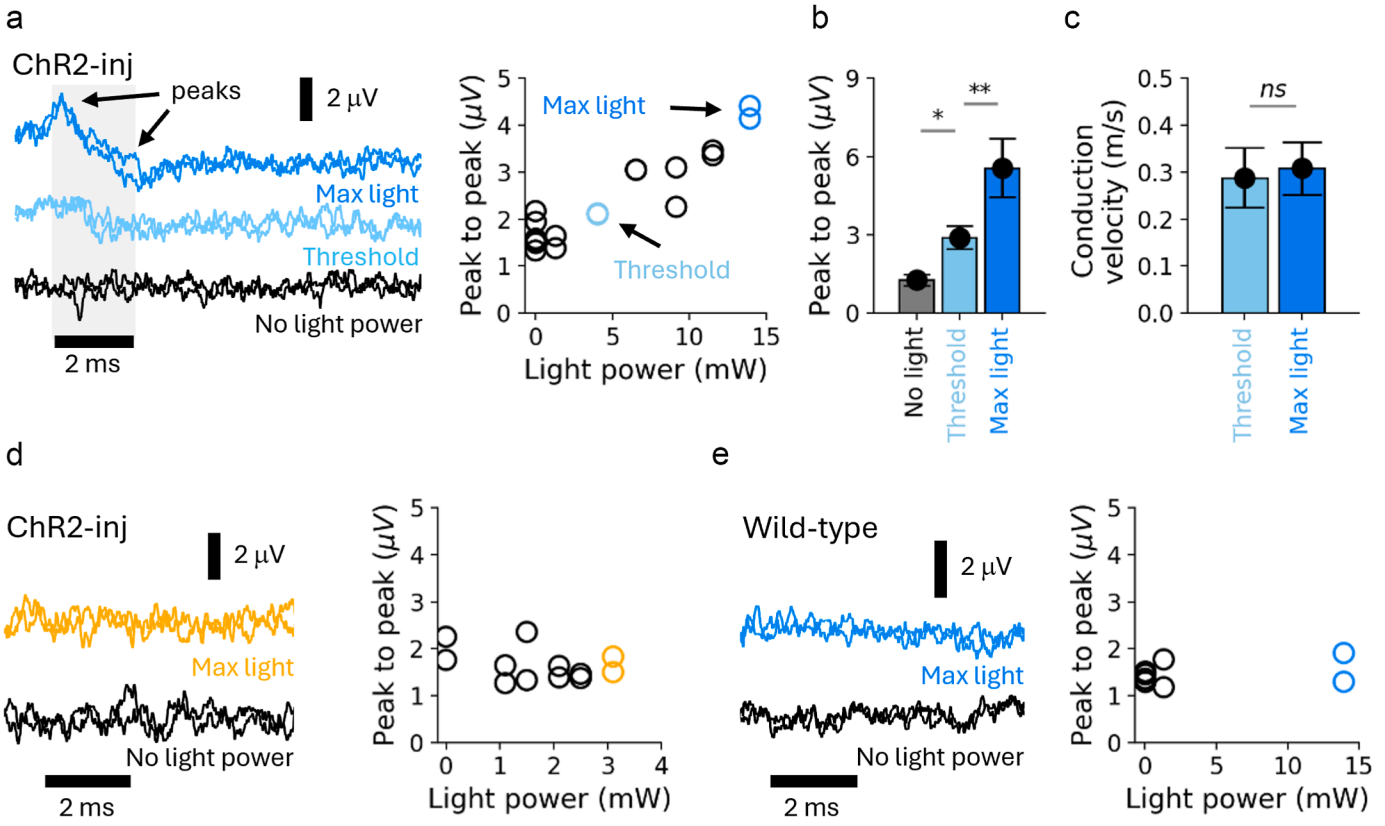

Figure 3. Blue-light–mediated *CAP*s in ChR2(H134R)-injected mice. *a.* Example CAP recordings (left) from one mouse injected with AAV6-ChR2(H134R) ("ChR2-inj") in response to 2-millisecond pulses of 452 nm wavelength blue light (shaded gray region). Responses are shown for 0 μW, 4 μW ("threshold"), and 13.9 μW ("max") blue light. Input/output function (I/O) showing peak-to-peak amplitude plotted against light power (right). Each open circle indicates mean of 20 trials (two per power level). b. Bar graph showing mean response during no light, threshold light, or max light, data from $n = 8$ mice. c. Bar graph showing peak conduction velocity at threshold and max light, data from $n = 8$ mice. d. CAP recording from one ChR2-inj mouse in response to 2-millisecond pulse of 595 nm wavelength amber light (left) and I/O function showing peak-to-peak amplitude against light power (right). e. Same as in panel d, but from the noninjected (wild-type) side of a ChR2-inj mouse in response to 2-millisecond pulses of 452 nm wavelength blue light. For all, closed circles indicate mean; error bars indicate SEM; *ns* indicates $p > 0.05$, $^*p < 0.05$, $^{**}p < 0.01$, Wilcoxon signed-rank test. [Color figure can be viewed at www.neuromodulationjournal.org]

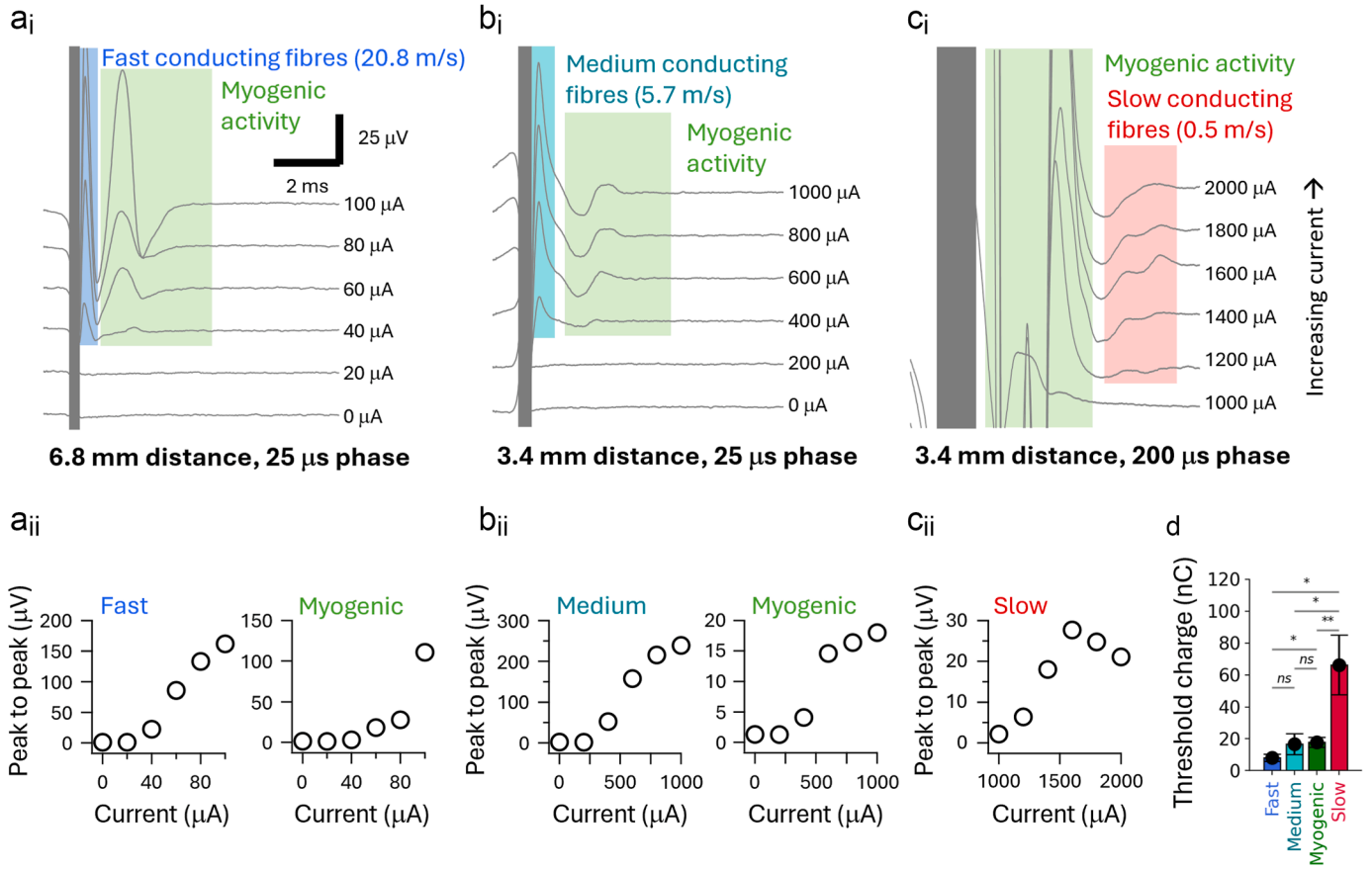

Figure 4. Electrical stimulation produces fast, medium and slow-conducting compound action potential and myogenic activity. a_i. Example recordings from one mouse showing eCAP responses to 25-millisecond pulse (8-millisecond interphase gap) at increasing current levels (distance between stimulating and recording electrodes = 6.8 mm). For each current, each trace is the average of 80 trials, half of which were elicited using reversed stimulating polarity. Stimulus artifact is blanked using gray bar. Responses show fast conducting, low threshold responses (blue box) and myogenic activity (green box). a_{ii}. Input/output (I/O) function showing peak-to-peak amplitude vs current level for fast fibers and myogenic activity identified in panel a_i. Each open circle indicates mean response across 80 trials (two blocks of 20 trials per current level, two stimulating configurations). b_i. Example recordings from the same animal as in panel a, showing eCAP responses to 25-millisecond pulse (8-millisecond interphase gap) at increasing current levels using a smaller distance between stimulating and recording electrodes (3.4 mm). Responses show medium conducting, moderate threshold responses (teal box) and myogenic activity (green box). b_{ii}. I/O function for each fiber class identified in panel b_i. c_i. Example recordings from the same animal as in panels a and b, showing eCAP responses to 200-millisecond pulse (50-millisecond interphase gap) at increasing current levels (distance between stimulating and recording electrodes = 3.4 mm). Responses show slow conducting high threshold responses (red box) and myogenic activity (green box). c_{ii}. I/O function for slow velocity fiber class in panel c_i. d. Bar graph showing summary data of threshold charge for each recorded fiber type. Closed circles indicate mean; error bars indicate SEM; *ns* indicates $p > 0.05$, $^*p < 0.05$, $^{**}p < 0.01$, post hoc Mann-Whitney U test. [Color figure can be viewed at www.neuromodulationjournal.org]

ChR2-H134R and eNpHR Expression in Small-Diameter, Slow Conducting Fiber Types

The sciatic nerve is a mixed somatic nerve that contains a variety of afferent (and efferent) fiber types, typically classified into fast, large-diameter myelinated fibers responsible for proprioceptive inputs (Aα fibers) and cutaneous mechanoreceptors (Aβ fibers), moderately fast, myelinated medium-diameter fibers responsible for sharp pain (Aδ fibers), and slow, unmyelinated small-diameter fibers for diffuse pain (C fibers).[30–32] In this study, slow velocity C fibers (in mice, reported between 0.2 and 1.3 m/s) were targeted for genetic modification using the viral serotype AAV6, which has a recognized propensity to target small-diameter nociceptors in the DRG.[15,17,31] Our histological and electrophysiological data support these findings, in which only small-diameter DRG cells expressed the opsin (identified using an attached fluorophore), compared with, for example, large-diameter mechanoreceptors, and the recorded conduction velocity of blue-light mediated responses in mice transduced with the excitatory ChR2-H134R were confirmed to be slow. Similarly to a previous report, we observed opsin-dependent variation in expression (ChR2-H134R+ expressed in <1% of cells with a mean soma size 182 µm^2; eNpHR-eYFP+ expressed in >7% of cells with a mean soma size 237 µm^2).[17] The reasons for this difference are not known but may relate to the individual viral preparation or some form of toxicity resulting from expression of the ChR2-H134R opsin, although toxicity has not been previously documented, at least in large-diameter fibers.[13]

Histological analysis revealed eNpHR-eYFP was expressed in a minimum of 7.1% of the total NeuN+ DRG population. Interestingly, only 50% of eNpHR+ cells colocalized with NeuN+, although there was no difference in size between NeuN+ and NeuN– cells. This suggests that eNpHR is expressed in small-diameter neurons (and not glia), and NeuN may not be an effective pan-neuronal marker for the mouse DRG. Therefore, we believe that 7% is only an estimation of total opsin expression. A study using a similar viral

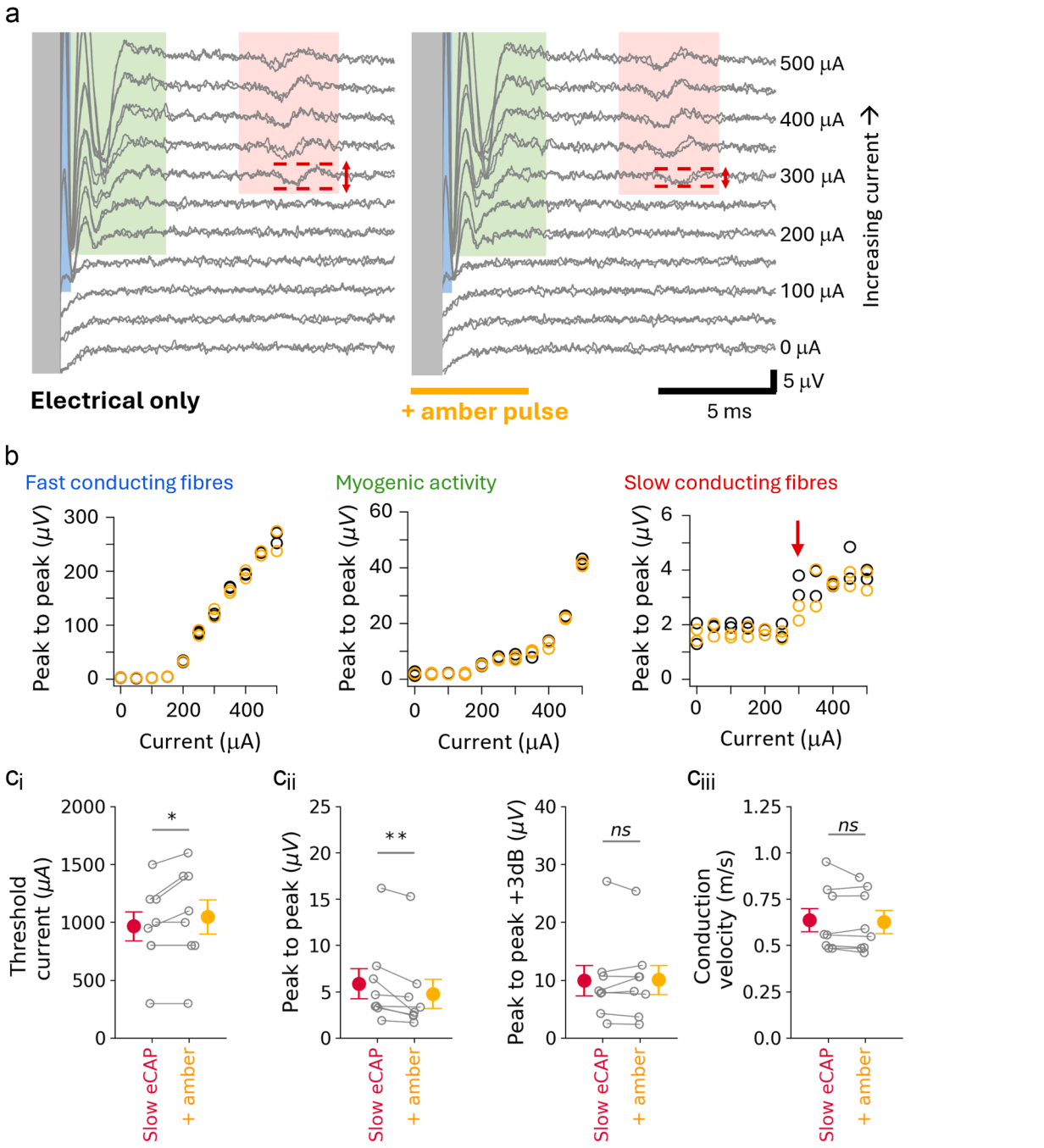

Figure 5. Amber light reduces slow conducting electrically evoked CAP responses. a. Example recording from one mouse injected with AAV6-eNpHR showing eCAP responses to 25-millisecond (8-millisecond interphase gap) increasing current levels without amber light (left) and with a 5-millisecond pulse of 595 nm amber light (right). Each trace is the average of 20 trials (two per current level). Fast, myogenic, and slow eCAPs are highlighted in blue, green, and red, respectively. b. Input/output functions for each fiber type from the same mouse as in panel a are shown without amber light (black open circles) and with amber light (orange open circles). Open circles indicate mean response over 20 trials (two blocks of 20 trials per current). c. Bar graphs showing summary data (n = 8 mice) showing slow eCAP threshold current (c_i), peak-to-peak response at threshold electrical stimulus (c_{ii} left), and 3 dB suprathreshold electrical stimulus (c_{ii} right) and conduction velocity (c_{iii}) in the absence (red) and presence (orange) of amber light. For all, open circles indicate individual mice; closed circles indicate mean; error bars indicate SEM; *ns* indicates $p > 0.05$, *$p < 0.05$, **$p < 0.01$, Wilcoxon signed-rank test. [Color figure can be viewed at www.neuromodulationjournal.org]

vector (AAV2/6) and injection approach reported an overall 16.5% eNpHR transduction, with 75% of neurons <200 µm^2.[17] Moreover, as in Iyer et al, a quarter of eNpHR+ cells colocalized with the peptidergic marker CGRP, suggesting a heterogeneous nociceptor population that was targeted by the AAV2/6. CGRP expression has been found to be associated with visceral afferents compared with cutaneous afferents, whereas nonpeptidergic markers such as isolectin B4 (IB4) are more prominent in the skin.[33] It should be noted that CGRP is not exclusive to peptidergic neurons and is present in Aδ fibers. One-fifth of eNpHR-eYFP positive cells

colocalized with mechanoreceptor marker NF200, although NF200 is not an exclusive marker of mechanoreceptors and also is present in Aδ fibers.[21] Many eNpHR cells (59%, mean soma size of 207 μm^2) did not colocalize with either the CGRP or NF200 marker. Although additional nociceptor markers (eg, transient receptor potential vanilloid 1 [TRPV1], substance P [SP], IB4) would assist in further confirming the selectivity of expression in nociceptors, we could not obtain reliable IB4 staining in this data set.[17,34] However, a previous study (using the same viral preparation) showed no selective targeting of one type of nociceptors over another.[17]

We further classified the AAV6 transduced neurons using conduction velocity through an excitatory opsin. In electrophysiological experiments in anaesthetized mice, we used pulses of blue light applied to the sciatic nerve to selectively activate those axons expressing ChR2-H134R. Despite the low expression of the opsin (~1% of the total NeuN population), blue-light stimulation elicited a small but robust single-peak, slow-velocity (0.3 m/s) response in all eight mice. These experiments further confirmed the propensity of AAV6 to target slow velocity C fibers.[15,17,18] We have, for what we believe is the first time, characterized the in vivo electrophysiological properties of ChR2-H134R expressed in slow velocity fibers in anesthetized mice. Collectively, our data suggest that the AAV6-hSyn is highly selective for slow conducting nociceptors.

Broadly, viral serotypes have been used to target functionally distinct neural populations. For example, AAV6 is well established to target small-diameter nociceptors[15,17,19] whereas AAV9 has been used successfully to target large-diameter mechanoreceptors.[13,19,20] Indeed, in our study, 75% of NpHR+ cells had soma sizes <267 μm^2. Moreover, blue-light stimulation of ChR2 (as the viral control group) did not elicit detectable fast CAP responses or visible muscle contraction. However, a minority of cells were larger diameter and coexpressed with NF200, and therefore are probably myelinated. This leads to the possibility that a small number of other myelinated axons (eg, efferent motor neurons) also may express the opsin. Although we did not evaluate the ventral root or spinal cord for opsin expression in motor fibers, a previous study using the same viral preparation has shown only occasional NpHR expression in motor axons projecting to sciatic adjacent muscles and attributed this to viral spillover into the cavity at injection.[17]

Because electrically evoked myogenic activity was unchanged between light-on and light-off conditions, we do not believe a large population of motor axons were transduced. However, future studies should evaluate and further quantify off-target expression, especially important to ensure selectivity of the neuromodulation in a clinical setting.

Using Optogenetics to Selectively Inhibit Slow Velocity Fiber Activity

Across cohorts, electrical stimulation reliably elicited multiphasic eCAP responses which, based on conduction velocity, could be delineated into fast Aβ, medium Aδ, or slow C fiber activity, in addition to myogenic activity. Optogenetic suppression was observed in slow velocity eCAPs (with a ~20% reduction across eight mice) but not in fibers with faster conducting or myogenic activity. This is in line with the highly selective expression pattern of eNpHR-eYFP (most of which was in small-diameter fibers likely to be nociceptors) and the velocity of optical responses measured in ChR2-H134R animals (0.3 m/s, in line with nociceptors). These data indicate that the suppression of neural activity is highly selective; thus, selective optogenetic inhibition should allow touch and proprioceptive activity to proceed normally.

To our knowledge, this is the first study to indicate optogenetic suppression of activity in sciatic nerve nociceptors through light delivered directly to, and recording from, the nerve trunk. Increases in slow velocity eCAP threshold and reductions in response amplitude were observed in the presence of amber light in some but not all mice, showing proof of concept but also highlighting significant challenges for potential applications and key future research directions. For example, the effectiveness of the eNpHR may be underestimated in this study because of the short pulse duration of amber light.[20] Using longer applications of light (eg, seconds or minutes) could be more effective, although rebound effects after light termination should be considered.[35]

Here, we have shown proof of principle that short but repetitive pulses of light can effectively reduce approximately 20% of electrically evoked nociceptive activity. This restricted use of light reduces the power demand and improves the power efficiency of potential clinical devices that will enable translation. However, future experiments should investigate the most effective and efficient modes of light delivery to inhibit nociceptors, particularly regarding behavioral outcomes.

The level of reduction in eCAP amplitude is dependent on a range of factors, including overall transduction efficiency and selectivity. Interestingly, we found no relationship between opsin expression and change in response amplitude or threshold, suggesting overall inhibition may depend on other factors, including the method used to activate or detect nociceptor activity. In addition, we did not show the specificity of eNpHR-mediated suppression to amber-light stimulation (eg, by comparing any effect of blue-light stimulation), although previous studies have shown no off-spectrum light effects.[17]

In this study, a strong electrical stimulus was necessary to evoke synchronized nociceptor activity that, although not physiological in nature, was required to elicit a detectable response. Importantly, suppression was only observed at threshold (ie, the minimum level of current needed to elicit slow eCAPs), and not at higher electrical levels. Because nociceptors are increasingly recruited and synchronized at suprathreshold current intensities, these fibers may be less susceptible to small inhibitory currents. Moreover, the spot size of amber stimulation is smaller than the area of the nerve. As electrical stimulation becomes widespread through the cross section of the nerve, the amber light is only able to activate a small number of opsin-positive cells directly in the path of the light, leaving the rest of the population unaffected.

The relatively asynchronous firing and slow conduction of C fibers make eCAPs harder to detect than faster conducting fibers, especially over longer distances. Therefore, it is possible that optogenetic inhibition may not be suppressing slow eCAP activity but rather desynchronizing them, which may manifest as a reduction in amplitude. We tested this by stimulating at two distances (3.4 and 6.8 mm) away from the recording electrode. Although we found no difference in eCAP response amplitude between distances, we also found no difference in the reduction of the response during amber-light stimulation (as a percentage). Further verification through multiunit spinal activity evoked by noxious stimuli at the paw, with and without light application to the nerve trunk, would provide a more physiological assessment of the impact of the optogenetic stimulation.[36,37]

Finally, to determine the physiological impact of nociceptor suppression, and to ascertain the safety of viral delivery, an implantable nerve cuff will be required to deliver light directly to the nerve trunk[38,39] to allow a behavioral assessment of sensitivity to pain, such as mechanical or thermal stimulation of the pain after a spared nerve injury or inflammatory pain model. In this scenario, a more realistic recruitment of nociceptive afferents may be used, as opposed to artificial electrical stimulation.

Although we have quantified the effect of optogenetic suppression of sciatic nerve nociceptors in isoflurane-anesthetized mice, this may be different in awake animals. Future long-term experiments, using long-term implanted devices capable of optical and electrical stimulation, in addition to electrophysiological recording capabilities, should be conducted across a range of behavioral stages (eg, asleep, quiet restfulness, and attentive states). These experiments also should investigate the light stimulation paradigms that produce the greatest effect while minimizing power demands.

The Site of the Sciatic Trunk for Optogenetic Inhibition

Optogenetic inhibition of action potential propagation has been shown in sciatic nerve motor fibers[38,40] and large-diameter sensory fibers,[20,41] but to our knowledge, there are no reports of similar nerve trunk inhibition of nociceptors. Transdermal application of light for optogenetic inhibition of nociceptor activity has been revealed in multiple studies through the use of behavioral responses to mechanical or thermal stimulation of the foot after the induction of a pain model.[14,17,41–43] These studies used three types of inhibitory opsins, the proton pump Arch (archaerhodopsin-3 from *Halorubrum sodomense*), its variant ArchT (archaerhodopsin from *Halorubrum* strain TP009), and chloride pump eNpHR.[44] The authors used a variety of genetic tools to express opsins within varying nociceptor classes (eg, TRPV1+, CGRP+), including AAV transduction[14,17,41] and transgenic mouse lines.[43] In these behavioral studies, measures of hypersensitivity (eg, through Von Frey mechanical, Hargreaves thermal) were used to assess the effectiveness of optogenetic inhibition after the induction of a pain model (eg, spared nerve injury).[17,41,43] Transdermal application of light to the foot was effective in suppressing pain perception, as measured by rescuing mechanical and thermal hypersensitivity, with one study estimating up to 73% increase in thermal thresholds.[17] In these studies, it could be argued that the light is preventing the initiation of action potentials in the nociceptors rather than suppressing activity that is already initiated. In the present study, light was applied to the nerve trunk, positioned between the stimulating and recording electrodes. With a spot size of 537 μm, we believe that the amber light is distinct from the site of initiation of action potentials and is therefore blocking the propagation of action potentials rather than preventing their initiation.

Clinical Considerations

Although optogenetics is largely used for the study of neural circuits, there is considerable interest in the clinical application of this technology.[45,46] Clinical trials are underway to test the safety and tolerability of opsin expression in the human retina for the restoration of vision (eg, Allergan, RST-001 NCT02556736), with promising functional outcomes.[47] Here, we have used an intrasciatic injection of AAVs to deliver opsins to the target tissue, although intra-DRG and intramuscular injections also have been used to similar effect.[15,48,49] Because there are known challenges of viral delivery for the delivery and expression of opsins in the human periphery,[50] future preclinical experiments should address immune responses and long-term safety of opsin after viral delivery. Future improvements in genetic tools (eg, using designer opsins, more targeted serotypes and/or promotors) may combat issues with immune responses, and improve selectivity to target tissues before clinical implementation, ensuring the long-term safety and effectiveness for robust neuromodulation in a clinical setting.

Effective optogenetic suppression of nociceptor activity is reliant on transduction of the specific population of nociceptors that is affected by hyperactivity arising from chronic pain. This is a very different scenario to electrical stimulation for the treatment of chronic pain, which, by targeting the afferent population (eg, Aβ, C), can suppress the transmission of nociceptor activity through gating mechanisms and/or use-dependent blocking, provided it is part of the same peripheral nerve circuit.[51] A previous study has reported an approximately 16% transduction rate of NpHR in nociceptors, which caused a remarkable improvement (>70%) in sensitivity thresholds measured in a chronic pain model.[17] Using optogenetic suppression, if only a fraction (in our study, ~7%) of the affected nociceptor population is transduced, optogenetic inhibition will have a limited but potentially significant impact. However, it is important to note that complete nociceptor inhibition is not desirable in a clinical setting, given pain plays an important role in alerting the individual to potential injury and to prevent further damage.

The electrical nerve cuff used in this study has been implanted long term in rodents, and modified versions have been used in sheep studies.[26,52] Clinical implementation of selective optogenetic suppression would require the development of a flexible nerve device with light emitters. Significant multidisciplinary research has emerged to address this for peripheral nerves.[53–56]

CONCLUSIONS

Our data indicate that light stimulation of eNpHR-eYFP at the level of the sciatic nerve trunk suppressed the amplitude of slow velocity eCAP responses. This study extends the current understanding of optogenetic approaches for selective inhibition of nociceptors to the level of the axon, combined with our approach to simultaneously monitoring neural activity. Understanding the underlying neural activity during inhibition of nociceptor activity is critical and may provide insights into developing new therapeutic strategies for managing chronic pain in humans.

Acknowledgements

The authors acknowledge the assistance and technical expertise of Jenny Zhou for fabrication of electrical nerve cuffs; Ella P. Trang, Patrick Lam, and Philippa Kammerer for tissue sectioning and antibody staining; Trung Nguyen for surgical advice, and James Firth and Joshua McLaughlin for anesthesia and animal monitoring.

Data Availability

The data that support the findings of this study are available from the corresponding author on reasonable request.

Authorship Statements

Mary G. Ardren was responsible for data curation, formal analysis, methods, software development, data interpretation, validation and visualization, original draft preparation, and reviewing and editing manuscripts. Jerico V. Matarazzo was responsible for data curation, software development, and reviewing and editing manuscripts. Elise A. Ajay was responsible for methods, software development, and reviewing and editing manuscripts. Alex C. Thompson was responsible for software development and reviewing and editing manuscripts. Sophie C. Payne was responsible for methods and reviewing and editing manuscripts. James B. Fallon was responsible for methods, data interpretation, and reviewing and editing manuscripts. Rachael T. Richardson was responsible for conceptualization, funding acquisition, methods, data interpretation, project administration, original draft preparation, and review and editing manuscripts. All authors approved the final manuscript.

Conflict of Interest

The authors reported no conflict of interest.

How to Cite This Article

Ardren M.G., Matarazzo J.V., Ajay E.A., Thompson A.C., Payne S.C., Fallon J.B., Richardson R.T. 2025. Selective Optogenetic Inhibition of Slow Conducting Fibers at the Level of the Sciatic Nerve Trunk in the Mouse. Neuromodulation 2025; ■: 1–13.

SUPPLEMENTARY DATA

To access the supplementary material accompanying this article, visit the online version of *Neuromodulation: Technology at the Neural Interface* at www.neuromodulationjournal.org and at https://doi.org/10.1016/j.neurom.2025.09.304.

REFERENCES

1. Deer T, Pope J, Benyamin R, et al. Prospective, multicenter, randomized, double-blinded, partial crossover study to assess the safety and efficacy of the novel neuromodulation system in the treatment of patients with chronic pain of peripheral nerve origin. *Neuromodulation*. 2016;19:91–100. https://doi.org/10.1111/ner.12381
2. Helm S, Shirsat N, Calodney A, et al. Peripheral nerve stimulation for chronic pain: a systematic review of effectiveness and safety. *Pain Ther*. 2021;10:985–1002. https://doi.org/10.1007/s40122-021-00306-4
3. Van Calenbergh F, Gybels J, Van Laere K, et al. Long term clinical outcome of peripheral nerve stimulation in patients with chronic peripheral neuropathic pain. *Surg Neurol*. 2009;72:330–335 [discussion: 335]. https://doi.org/10.1016/j.surneu.2009.03.006
4. Todd AJ. Neuronal circuitry for pain processing in the dorsal horn. *Nat Rev Neurosci*. 2010;11:823–836. https://doi.org/10.1038/nrn2947
5. Sheikh N, Dua A. *Neuroanatomy, Substantia Gelatinosa*. StatPearls Publishing; 2025
6. Smith KM, Browne TJ, Davis OC, et al. Calretinin positive neurons form an excitatory amplifier network in the spinal cord dorsal horn. *eLife*. 2019;8:e49190. https://doi.org/10.7554/eLife.49190
7. Finch P, Price L, Drummond P. High-frequency (10 kHz) electrical stimulation of peripheral nerves for treating chronic pain: a double-blind trial of presence vs absence of stimulation. *Neuromodulation Technol Neural Interface*. 2019;22:529–536. https://doi.org/10.1111/ner.12877
8. Kapural L, Yu C, Doust MW, et al. Novel 10-kHz high-frequency therapy (HF10 therapy) is superior to traditional low-frequency spinal cord stimulation for the treatment of chronic back and leg pain: the SENZA-RCT randomized controlled trial. *Anesthesiology*. 2015;123:851–860. https://doi.org/10.1097/ALN.0000000000000774
9. Patel YA, Butera RJ. Differential fiber-specific block of nerve conduction in mammalian peripheral nerves using kilohertz electrical stimulation. *J Neurophysiol*. 2015;113:3923–3929. https://doi.org/10.1152/jn.00529.2014
10. Deisseroth K. Optogenetics: 10 years of microbial opsins in neuroscience. *Nat Neurosci*. 2015;18:1213–1225. https://doi.org/10.1038/nn.4091
11. Nagel G, Brauner M, Liewald JF, Adeishvili N, Bamberg E, Gottschalk A. Light activation of Channelrhodopsin-2 in excitable cells of Caenorhabditis elegans triggers rapid behavioral responses. *Curr Biol*. 2005;15:2279–2284. https://doi.org/10.1016/j.cub.2005.11.032
12. Gradinaru V, Thompson KR, Deisseroth K. eNpHR: a Natronomonas halorhodopsin enhanced for optogenetic applications. *Brain Cell Biol*. 2008;36:129–139. https://doi.org/10.1007/s11068-008-9027-6
13. Kubota S, Sidikejiang W, Kudo M, et al. Optogenetic recruitment of spinal reflex pathways from large-diameter primary afferents in non-transgenic rats transduced with AAV9/channelrhodopsin 2. *J Physiol*. 2019;597:5025–5040. https://doi.org/10.1113/JP278292
14. Li B, Yang XY, Qian FP, Tang M, Ma C, Chiang LY. A novel analgesic approach to optogenetically and specifically inhibit pain transmission using TRPV1 promoter. *Brain Res*. 2015;1609:12–20. https://doi.org/10.1016/j.brainres.2015.03.008
15. Towne C, Pertin M, Beggah AT, Aebischer P, Decosterd I. Recombinant adeno-associated virus serotype 6 (rAAV2/6)-mediated gene transfer to nociceptive neurons through different routes of delivery. *Mol Pain*. 2009;5:52. https://doi.org/10.1186/1744-8069-5-52
16. Alberio L, Locarno A, Saponaro A, et al. A light-gated potassium channel for sustained neuronal inhibition. *Nat Methods*. 2018;15:969–976. https://doi.org/10.1038/s41592-018-0186-9
17. Iyer SM, Montgomery KL, Towne C, et al. Virally mediated optogenetic excitation and inhibition of pain in freely moving nontransgenic mice. *Nat Biotechnol*. 2014;32:274–278. https://doi.org/10.1038/nbt.2834
18. Iyer SM, Vesuna S, Ramakrishnan C, et al. Optogenetic and chemogenetic strategies for sustained inhibition of pain. *Sci Rep*. 2016;6:30570. https://doi.org/10.1038/srep30570
19. Kudo M, Wupuer S, Fujiwara M, et al. Specific gene expression in unmyelinated dorsal root ganglion neurons in nonhuman primates by intra-nerve injection of AAV 6 vector. *Mol Ther Methods Clin Dev*. 2021;23:11–22. https://doi.org/10.1016/j.omtm.2021.07.009
20. Kosugi A, Kudo M, Inoue KI, Takada M, Seki K. Bidirectional optogenetic modulation of peripheral sensory nerve activity: induction vs. suppression through channelrhodopsin and halorhodopsin. *iScience*. 2025;28:112178. https://doi.org/10.1016/j.isci.2025.112178
21. Espinosa-Juárez JV, Chiquete E, Estañol B, Aceves JJ. Optogenetic and chemogenic control of pain signaling: molecular markers. *Int J Mol Sci*. 2023;24:10220. https://doi.org/10.3390/ijms241210220
22. Matarazzo JV, Ajay EA, Payne SC, et al. Combined optogenetic and electrical stimulation of the sciatic nerve for selective control of sensory fibers. *Front Neurosci*. 2023;17:1190662. https://doi.org/10.3389/fnins.2023.1190662
23. Ecanow A, Berglund K, Carrasco D, Isaacson R, English AW. Enhancing motor and sensory axon regeneration after peripheral nerve injury using bioluminescent optogenetics. *Int J Mol Sci*. 2022;23:16084. https://doi.org/10.3390/ijms232416084
24. Yang OJ, Robilotto GL, Alom F, et al. Evaluating the transduction efficiency of systemically delivered AAV vectors in the rat nervous system. *Front Neurosci*. 2023;17, 1001007. https://doi.org/10.3389/fnins.2023.1001007
25. Villalobos J, Payne SC, Ward GM, et al. Stimulation parameters for directional vagus nerve stimulation. *Bioelectron Med*. 2023;9:16. https://doi.org/10.1186/s42234-023-00117-2
26. Payne SC, Ward G, Fallon JB, et al. Blood glucose modulation and safety of efferent vagus nerve stimulation in a type 2 diabetic rat model. *Physiol Rep*. 2022;10:e15257. https://doi.org/10.14814/phy2.15257
27. Fallon JB, Senn P, Thompson AC. A highly configurable neurostimulator for chronic pre-clinical stimulation studies. In: *Proceedings of the Neural Interfaces Conferences*. 2018
28. Ajay EA, Trang EP, Thompson AC, et al. Auditory nerve responses to combined optogenetic and electrical stimulation in chronically deaf mice. *J Neural Eng*. 2023;20:026035. https://doi.org/10.1088/1741-2552/acc75f
29. Fallon JB, Payne SC. Electrophysiological recording of electrically-evoked compound action potentials. Accessed April 7, 2025. https://www.protocols.io/view/electrophysiological-recording-of-electrically-evo-yxmvmxmp9l3p/v1
30. Ruscheweyh R, Forsthuber L, Schoffnegger D, Sandkühler J. Modification of classical neurochemical markers in identified primary afferent neurons with Aβ-, Aδ-, and C-fibers after chronic constriction injury in mice. *J Comp Neurol*. 2007;502:325–336. https://doi.org/10.1002/cne.21311
31. Cain DM, Khasabov SG, Simone DA. Response properties of mechanoreceptors and nociceptors in mouse glabrous skin: an in vivo study. *J Neurophysiol*. 2001;85:1561–1574. https://doi.org/10.1152/jn.2001.85.4.1561
32. Steffens H, Dibaj P, Schomburg ED. In vivo measurement of conduction velocities in afferent and efferent nerve fibre groups in mice. *Physiol Res*. 2012;61:203–214. https://doi.org/10.33549/physiolres.932248

33. Bennett DLH, Dmietrieva N, Priestley JV, Clary D, McMahon SB. trkA, CGRP and IB4 expression in retrogradely labelled cutaneous and visceral primary sensory neurones in the rat. *Neurosci Lett*. 1996;206:33–36. https://doi.org/10.1016/0304-3940(96)12418-6
34. Payne SC, Belleville PJ, Keast JR. Regeneration of sensory but not motor axons following visceral nerve injury. *Exp Neurol*. 2015;266:127–142. https://doi.org/10.1016/j.expneurol.2015.02.026
35. Parrish RR, MacKenzie-Gray Scott C, Jackson-Taylor T, et al. Indirect effects of halorhodopsin activation: potassium redistribution, nonspecific inhibition, and spreading depolarization. *J Neurosci*. 2023;43:685–692. https://doi.org/10.1523/JNEUROSCI.1141-22.2022
36. Sales AC, Newton GWT, Pickering AE, Dunham JP. Multisite silicon probes enable simultaneous recording of spontaneous and evoked activity in multiple isolated C-fibres in rat saphenous nerve. *J Neurosci Methods*. 2022;368:109419. https://doi.org/10.1016/j.jneumeth.2021.109419
37. Su TF, Hamilton JD, Guo Y, et al. Peripheral direct current reduces naturally evoked nociceptive activity at the spinal cord in rodent models of pain. *J Neural Eng*. 2024;21:026044. https://doi.org/10.1088/1741-2552/ad3b6c
38. Michoud F, Sottas L, Browne LE, et al. Optical cuff for optogenetic control of the peripheral nervous system. *J Neural Eng*. 2018;15:015002. https://doi.org/10.1088/1741-2552/aa9126
39. Towne C, Montgomery KL, Iyer SM, Deisseroth K, Delp SL. Optogenetic control of targeted peripheral axons in freely moving animals. *PLoS One*. 2013;8, e72691. https://doi.org/10.1371/journal.pone.0072691
40. Liske H, Towne C, Anikeeva P, et al. Optical inhibition of motor nerve and muscle activity *in vivo*. *Muscle Nerve*. 2013;47:916–921. https://doi.org/10.1002/mus.23696
41. Boada DM, Martin TJ, Peters CM, et al. Fast-conducting mechanoreceptors contribute to withdrawal behavior in normal and nerve injured rats. *Pain*. 2014;155:2646–2655. https://doi.org/10.1016/j.pain.2014.09.030
42. Daou I, Beaudry H, Ase AR, et al. Optogenetic silencing of Nav1.8-positive afferents alleviates inflammatory and neuropathic pain. *eNeuro*. 2016;3ENEURO.0140-15.2016. https://doi.org/10.1523/ENEURO.0140-15.2016
43. Cowie AM, Moehring F, O'Hara C, Stucky CL. Optogenetic inhibition of CGRPα sensory neurons reveals their distinct roles in neuropathic and incisional pain. *J Neurosci*. 2018;38:5807–5825. https://doi.org/10.1523/JNEUROSCI.3565-17.2018
44. Guru A, Post RJ, Ho YY, Warden MR. Making sense of optogenetics. *Int J Neuropsychopharmacol*. 2015;18:pyv079. https://doi.org/10.1093/ijnp/pyv079
45. Bansal A, Shikha S, Zhang Y. Towards translational optogenetics. *Nat Biomed Eng*. 2023;7:349–369. https://doi.org/10.1038/s41551-021-00829-3
46. Boyle PM, Karathanos TV, Trayanova NA. '"Beauty is a light in the heart": the transformative potential of optogenetics for clinical applications in cardiovascular medicine'. *Trends Cardiovasc Med*. 2015;25:73–81. https://doi.org/10.1016/j.tcm.2014.10.004
47. Sahel JA, Boulanger-Scemama E, Pagot C, et al. Partial recovery of visual function in a blind patient after optogenetic therapy. *Nat Med*. 2021;27:1223–1229. https://doi.org/10.1038/s41591-021-01351-4
48. Glatzel M, Flechsig E, Navarro B, et al. Adenoviral and adeno-associated viral transfer of genes to the peripheral nervous system. *Proc Natl Acad Sci U S A*. 2000;97:442–447. https://doi.org/10.1073/pnas.97.1.442
49. Yu H, Fischer G, Ferhatovic L, et al. Intraganglionic AAV6 results in efficient and long-term gene transfer to peripheral sensory nervous system in adult rats. *PLoS One*. 2013;8, e61266. https://doi.org/10.1371/journal.pone.0061266
50. Maimon BE, Diaz M, Revol ECM, et al. Optogenetic peripheral nerve immunogenicity. *Sci Rep*. 2018;8:14076. https://doi.org/10.1038/s41598-018-32075-0
51. Zhang S, Chen L, Ladez SR, Seferge A, Liu J, Feng B. Blocking Aδ- and C-fiber neural transmission by sub-kilohertz peripheral nerve stimulation. *Front Neurosci*. 2024;18:1404903. https://doi.org/10.3389/fnins.2024.1404903
52. Payne SC, Burns O, Stebbing M, et al. Vagus nerve stimulation to treat inflammatory bowel disease: a chronic, preclinical safety study in sheep. *Bioelectron Med*. 2018;1:235–250. https://doi.org/10.2217/bem-2018-0011
53. Kim D, Yokota T, Suzuki T, et al. Ultraflexible organic light-emitting diodes for optogenetic nerve stimulation. *Proc Natl Acad Sci U S A*. 2020;117:21138–21146. https://doi.org/10.1073/pnas.2007395117
54. Song KI, Park SE, Lee S, Kim H, Lee SH, Youn I. Compact optical nerve cuff electrode for simultaneous neural activity monitoring and optogenetic stimulation of peripheral nerves. *Sci Rep*. 2018;8:15630. https://doi.org/10.1038/s41598-018-33695-2
55. Zhang Y, Mickle AD, Gutruf P, et al. Battery-free, fully implantable optofluidic cuff system for wireless optogenetic and pharmacological neuromodulation of peripheral nerves. *Sci Adv*. 2019;5:eaaw5296. https://doi.org/10.1126/sciadv.aaw5296
56. Zheng H, Zhang Z, Jiang S, et al. A shape-memory and spiral light-emitting device for precise multisite stimulation of nerve bundles. *Nat Commun*. 2019;10:2790. https://doi.org/10.1038/s41467-019-10418-3

COMMENT

These initial findings show successful inhibition of activity in peripheral nociceptive fibers in an intact animal model on light activation of the inhibitory opsin halorhodopsin, after its expression by the intraneural injection of a viral vector. This is an important step toward using optogenetic regulation to control function of peripheral sensory pathways for pain control.

Quinn H. Hogan, MD
Milwaukee, WI, USA